Design and performance of a polymer Mach-Zehnder interferometer electro-optic modulator at 1.55 μm*

ZHENG Chuan-tao (郑传涛)**, **LIANG Lei** (梁磊), **YAN Yun-fei** (闫云飞), **MA Chun-sheng** (马春生), and **ZHANG Da-ming** (张大明)

State Key Laboratory on Integrated Optoelectronics, College of Electronic Science and Engineering, Jilin University, Changchun 130012, China

(Received 2 January 2013)

Based on poled guest-host electro-optic (EO) polymer DR1/SU-8, a Mach-Zehnder interferometer (MZI) EO modulator operated at 1.55 μm is proposed. For achieving high response speed and high EO modulation efficiency, both waveguide structure and electrode structure are especially optimized. The impedance match and less index mismatch are achieved. The final characteristic impedance of electrode is about 49.4 Ω, and the microwave index and the lightwave index are 1.5616 and 1.6006, respectively. The device is fabricated using wet-etching technique and inductively coupled plasma (ICP) etching technique, and its performance is measured at 1.55 μm. Experimental results show that when the applied voltage is tuned, the modulator can be changed from ON state to OFF state. The insertion loss at ON state is 12 dB and the extinction ratio between ON and OFF states is about 10 dB. The high response speed is in nanosecond level for a square-wave signal. Therefore, the modulator possesses potential applications in high-speed optical networks on chip.

Document code: A **Article ID:** 1673-1905(2013)04-0254-5

DOI 10.1007/s11801-013-3003-9

Optical switches, modulators and attenuators are important components in optical networks on chip (ONoC), optical interconnects and millimeter and microwave photonics[1-4]. In order to get excellent performance, various electro-optic (EO) devices based on different waveguide structures including standard directional coupler (DC)[5], Y-fed coupler[6], Mach-Zehnder interferometer (MZI)[7], multimode interference (MMI) coupler[8] and phase-generating coupler (PGC)[9], as well as different electrode structures including four-section cross-connect microstrip line (MSL) electrode[5], two-section reversed electrodes[10] and shielded push-pull MSL electrode[11] have been proposed for decreasing driving voltage and speeding up response, minimizing insertion loss and crosstalk, and broadening lightwave spectrum.

The dye-doped EO polymers based on disperse red 1 (DR1) chromophore can be simply synthesized, and the related reported devices utilizing the guest-host polymer DR1/polymethyl methacrylate (PMMA) and side-chain polymer DR1-co-PMMA reveal some acceptable properties[12,13]. Besides PMMA, the negative tone photoresist SU-8 has good chemical and thermal stability and high optical transparency around 1.55 μm. In this paper, an MZI EO modulator based on synthesized guest-host EO polymer DR1/SU-8 is optimally designed and fabricated using wet-etching technique and inductively coupled plasma (ICP) etching technique. And owning to good impedance match and small refractive index mismatch, the device reveals high response speed of 16 ns.

The schematic diagram of the designed polymer MZI EO modulator is shown in Fig.1(a), which consists of a 3 dB Y-branch splitter, an MZI EO region and a 3 dB Y-branch combiner. The modulator is equipped with MSL electrode, which contains a pair of electrodes on two MZI arms and a grounded electrode. For increasing modulation bandwidth, the MSL electrode is configured to be traveling-wave style with a load resistance of Z_L=50 Ω. The length of EO active region is L_{EO}, and the gap between the two MZI arms is d. The electrode width and gap in the MZI region are W and G, respectively. The input power and output power are denoted by P_{in} and P_{out}, respectively.

The cross-section view of EO active region is shown in Fig.1(b). The poling directions of the two rib cores are opposite, as labeled in Fig.1(b). Silicon is used as substrate, the DR1 chromophore doped EO polymer DR1/SU-8 is used as core, the upper and under buffer layers and the layer besides the core are the same material of

* This work has been supported by the National Science Foundation Council of China (Nos.61107021, 61177027 and 61077041), the Ministry of Education of China (Nos.20110061120052 and 20120061130008), the China Postdoctoral Science Foundation Funded Project (Nos.20110491299 and 2012T50297), and the Special Funds of Basic Science and Technology of Jilin University (Nos.201103076 and 200905005).

** E-mail: zhengchuantao578@163.com

SU-8, the two upper driving electrodes and under grounded electrode are made of aluminum, and the upper confined layer upon the driving electrode is air. Under 1.55 μm, the optical coefficients of DR1/SU-8 are n_{10}= 1.620 and α_{10}=2.0 dB/cm, those of the buffer material SU-8 are n_{20}=1.573 and α_{20}=0.95 dB/cm, and those of the upper confined layer air are n_{40}=1.0 and α_{40}=0, respectively. The refractive index and bulk amplitude extinction coefficient of the aluminum are n_3=1.44 and κ_{30} =16.0, respectively. For realizing fundamental mode propagation and low optical loss, the waveguide parameters are optimized as a=3.0 μm, b_1=3.0 μm, b_2=3.0 μm, b_3=3.0 μm and b_4=0.1 μm. In this case, the effective refractive index and amplitude loss coefficient of E_{00}^{y} mode are n_{eff0}=1.6006 and α_{eff0}=1.9063 dB/cm, respectively. In the MZI EO region, the coupling coefficient between the two MZI arms should be weakened and neglected, so the coupling gap should be selected as large as possible. Here we choose d=30 μm, and the corresponding coupling coefficient K is below 1.39×10^{-14} m^{-1}. The EO active region length is L_{EO}=2.2 cm.

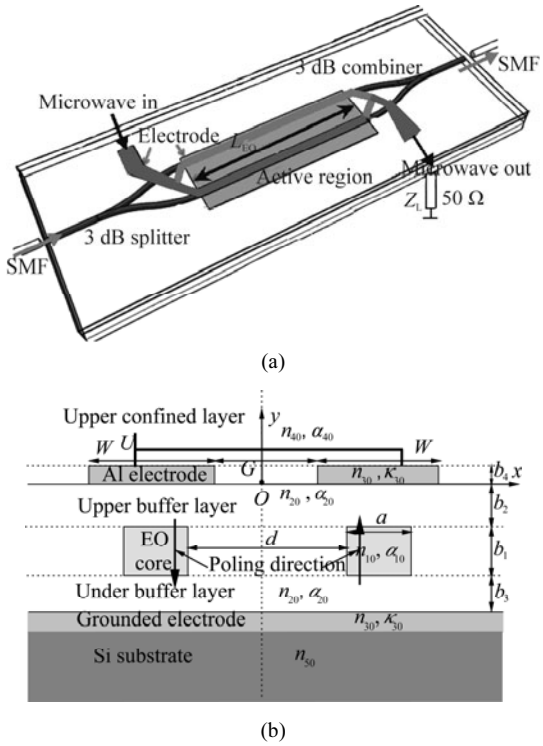

Fig.1 (a) Schematic diagram of the fabricated polymer MZI EO modulator; (b) Cross-section view in the EO active region, where SMF means single mode fiber

The electrodes on the layered dielectric medium shown in Fig.1(b) can be analyzed with extended point-matching method[14,15], and the detailed formulation can be seen in our previous report[11]. The electric potential distribution ϕ (V) and electric field component E_y (V/mm) over the cross-section region in Fig.1(b) are shown in Fig.2(a) and (b), respectively, where W =10 μm, G =25 μm, b_4 = 0.1 μm, and the applied voltages on the two upper electrodes are both 1 V. We observe that the electric field component E_y in the left core region and that in the right core region are identical in both direction and amplitude. Since the two cores are reversely poled, there will be a mismatch between the two mode propagation constants.

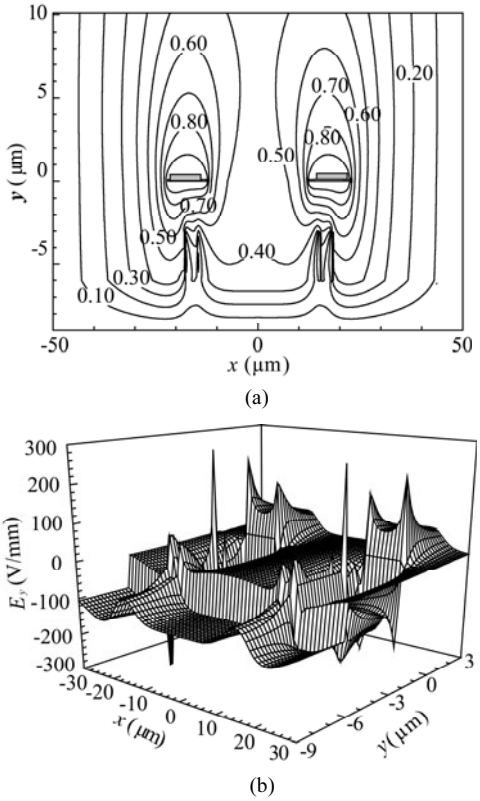

Fig.2 (a) Electric potential distribution and (b) electric field component E_y (V/mm) within the EO cross-section region, where W = 10 μm, G = 25 μm, b_4=0.1 μm and U = 1 V

Over the cross-section of waveguide, when the external electric field $E_y(x,y)$ is applied, the fundamental mode effective refractive index of one waveguide can be changed from n_{eff0} to $n_{\text{eff0}}+\Delta n_{\text{eff0}}$, that of another waveguide can be changed from n_{eff0} to $n_{\text{eff0}}-\Delta n_{\text{eff0}}$, and

$$\Delta n_{\text{eff0}} = -\frac{1}{2} n_1^3 \left(n_1/n_{\text{eff0}}\right) \gamma_{33} U \Gamma_y , \tag{1}$$

where the EO overlap integral Γ_y is given by

$$\Gamma_y = \frac{1}{U} \frac{\iint_{\text{core}} E_y(x,y) \left|E_{y0}(x,y)\right|^2 \mathrm{d}x\mathrm{d}y}{\iint_{-\infty}^{+\infty} \left|E_{y0}(x,y)\right|^2 \mathrm{d}x\mathrm{d}y} . \tag{2}$$

The propagation constant mismatch between the two waveguides is

$$\Delta\beta = \frac{2\pi}{\lambda}\left(n_{\text{eff0}} + \Delta n_{\text{eff0}}\right) - \frac{2\pi}{\lambda}\left(n_{\text{eff0}} - \Delta n_{\text{eff0}}\right) = 4\pi\Delta n_{\text{eff0}}/\lambda . \tag{3}$$

The output power of the modulator is

$$P_{\text{out}} = P_{\text{in}} \cos^2\left(\Delta\beta L_{\text{EO}}/2\right). \quad (4)$$

Then the output power can be modulated by the applied voltage. When U= 0 V, P_{out} becomes the maximum; whereas under an appreciate voltage named half-wave voltage, P_{out} becomes the minimum.

Still, the electrode should be treated as the distributed parameter circuit, and the microwave characteristic impedance and microwave effective refractive index are

$$Z_{\text{c}} = 1\Big/\left(c\sqrt{C_0 C_0^{'}}\right), \quad (5)$$

$$n_{\text{m}} = \sqrt{C_0/C_0^{'}}, \quad (6)$$

where $C_0 = \frac{1}{U}\oiint \varepsilon_0 \varepsilon \boldsymbol{E}\cdot \mathrm{d}\boldsymbol{S}$ is the capacity between one operation electrode and the grounded electrode, $\boldsymbol{E}'$ is the electric field surrounding the operation electrode, ε_0 is the permittivity in free space, and ε is the relative dielectric constant of the material surrounding the operation electrode. $C_0^{'}$ is the capacity of the same electrode when embedded in the free space, which can be similarly calculated with C_0.

The electrode dimensions (W and G) should be optimized to realize the high EO overlap integral and the good match between the characteristic impedance of electrode and load resistance. Noticing that the two operation electrodes combine at the microwave's input port and output port, each branch should possess a characteristic impedance of 100 Ω. Fig.3 shows the EO overlap integral Γ_y of one waveguide core, impedance Z_{c} for one electrode branch and microwave effective refractive index n_{m} versus the electrode dimension W with different G, where a=3.0 μm, b_1=3.0 μm, b_2=3.0 μm, b_3=3.0 μm and b_4=0.1 μm. From Fig.3(a), under certain W, as G increases from 5 μm to 30 μm, Γ_y increases and reaches the maximum value under G =25 μm. But as G increases to 30 μm, Γ_y decreases. Therefore, a suitable selection, for example, G =20 μm and W =10 μm, is desired for enhancing Γ_y. Meanwhile, from Fig.3(b), when G =10 μm and W =10.5 μm, the impedance for a single branch is Z_{c} =98.7 Ω. In this case, n_{m} =1.5616 exhibits a small mismatch with lightwave index of n_{eff0} =1.6006, and Γ_y=0.03431 μm^{-1}.

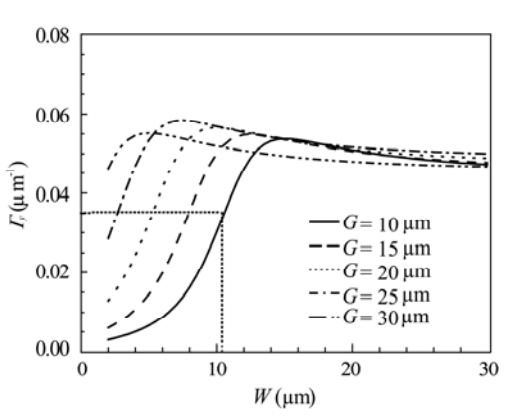

(a)

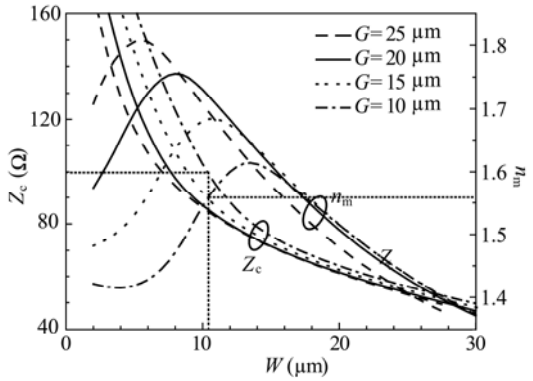

(b)

Fig.3 (a) EO overlap integral Γ_y for one waveguide core and (b) characteristic impedance Z_{C} for one branch and microwave effective refractive index n_{m} versus W with different G

The EO polymer material was synthesized using physical doping process by mixing 3% DR1 in thinner SU-8 and SU-8, and a proper amount of photoinitiator was added to the mixture for obtaining high stability in thermal and dipole alignment. The solution was stirred for 12 h under dark and thermostatic condition and filtered by a molecular sieve, and finally the EO material was obtained. The 5% weight loss temperature of SU-8 in N_2 atmosphere is about 320 ℃, and that of exposed DR1/SU-8 in N_2 atmosphere is about 297 ℃. During poling, the poling temperature is set to be 215 ℃.

A 3 μm-thick SU-8 was firstly spin-coated as lower cladding on Si substrate, which was cured following three steps, including soft bake at 90 ℃ for 1 min, exposure under ultraviolet (UV) light (350−400 nm) at 15 mW/cm^2 for 7 s, and hard bake at 150 ℃ for 10 min. In the next, another 3 μm-thick SU-8 was spin-coated and exposed to UV light through a contact chromium mask. The sample was developed for 1 min to form channels, and then hard baked. Thirdly, the EO polymer material was spin-coated, the two channels were filled, and soft bake, exposure and hard bake were used to cure the film sequentially. The slab on the top of the waveguide channels was removed by inductively coupled plasma (ICP) with 40 cm^3/min O_2 and 4 cm^3/min SF_4. The finally fabricated square waveguide is shown by the SEM photo in Fig.4, where the photo is taken in the MZI EO region. We see that the waveguide possesses good appearance. Finally, another SU-8 film as upper buffer was spin-coated and cured to cover the EO core.

Next, a 100 nm-thick aluminum layer was deposited through thermal evaporation. Then, the photoresist (BP212) was spin-coated and baked at 90 ℃ for 1 min. It was patterned by exposure with an electrode mask. To remove the photoresist and under aluminum, development was carried out in developer and NaOH solution successively. By using another exposure and development, all photoresist was removed, and the two driving electrodes were left. The fabricated device sample was contact-poled at

215 ℃ in N_2 atmosphere for 30 min.

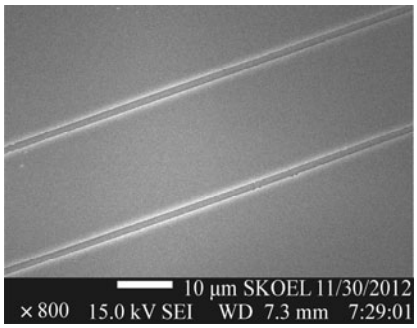

Fig.4 SEM photo of the fabricated square waveguides

The input power (1 mW/0 dBm, at 1.55 μm) generated by a tunable semiconductor laser (Santec, TSL-210) is coupled into the input waveguide of the modulator through a single mode fiber (SMF). The output power from the modulator is measured by an optical power meter. By tuning the applied voltage, the maximum output power under ON state is measured to be −12 dBm, which indicates that the insertion loss, including the propagation loss, bending loss and splitting loss, is about 12 dB. Whereas the minimum output power under OFF state is measured to be −22 dBm, which indicates that the extinction ratio between ON and OFF states is 10 dB.

The dynamic response is obtained by measuring the output electric signal generated by a high-speed photodiode detector, into which the output optical power is coupled through an output SMF. A square-wave alternative current (AC) signal with a frequency of 2 MHz is applied on the electrode through microwave probes, and the output signal from the detector is measured with a digital oscilloscope (Tektronix 2012B). The observed AC modulation signal and response signal are shown in Fig.5.

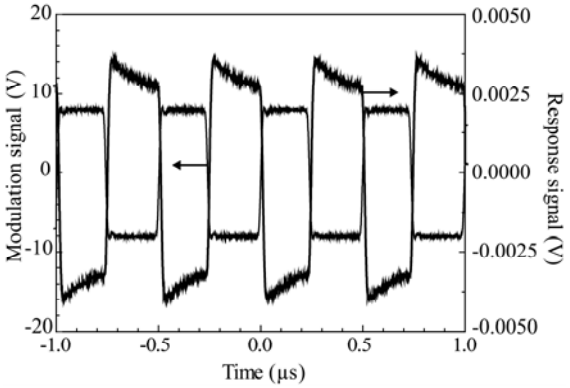

Fig.5 Detailed illustration of the measured modulation signal and response signal

The modulated response signal is then normalized for a clear observation, and the normalized output power values both in non-dB form and dB form from the modulator are shown in Fig.6. It can be observed that the extinction ratio between ON state and OFF state is larger than 10 dB. The 10%−90% rise time and fall time are characterized in detail in Fig.6. It can be determined that the rise time and fall time are about 15 ns and 16 ns, respectively.

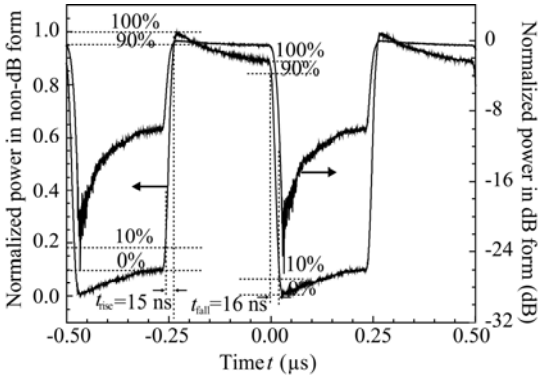

Fig.6 10%−90% response time characterization of the modulator

Comparisons are performed between the performance of this fabricated polymer EO modulator based on DR1/SU-8 and other reported EO modulators based on poled polymer materials. The results are depicted in Tab.1. We can see that this EO modulator exhibits some excellent features.

Tab.1 Comparisons between the performance of this fabricated polymer EO modulator and other reported EO modulators (*IL*: insertion loss; *ER*: extinction ratio; *RT*: response time)

Reference	Structure	EO polymer	*IL* (dB)	*ER* (dB)	*RT* (ns)
[2]	Directional coupler	Crosslinkable AJ309	15.0	-	-
[2]	Directional coupler	Guest-host AJLS102	10.4	6.7	-
[16]	Micro-ring resonator	Guest-host TCVDPA/SU-8	20	-	-
[11]	Symmetric MZI	Guest-host DR1/PMMA	-	20.7	-
This paper	Symmetric MZI	Guest-host DR1/SU-8	12	>10	~16

In conclusion, based on guest-host EO polymer DR1/SU-8, an MZI EO modulator with rectangular waveguide and MSL electrode is optimally designed using EO modulation theory and extended point-matching method, for realizing fundamental mode propagation, low optical loss, good impedance match, small refractive index mismatch and high EO modulation efficiency. The device is seriously fabricated using wet-etching technique and ICP etching technique. The insertion loss under ON state is about 12 dB, and the extinction ratio between ON state and OFF state is about 10 dB. Due to the impedance-matched electrode, small index mismatch and serious control on fabrication process, higher response speed (~16 ns) is observed.

References

[1] L. Liang, Y. Yan, X. Sun, C. Ma, D. Zhang and C. Zheng, J. Optoelectron. Laser **23**, 1246 (2012). (in Chinese)

[2] Y. Enami, D. Mathine, C. T. DeRose, R. A. Norwood, J. Luo, A. K. Y. Jen and N. Peyghambarian, Appl. Phys. Lett. **94**, 213513 (2009).

[3] Y. H. Lin, J. K. Li, T. Y. Chu and H. K. Hsu, Opt. Express **18**, 10104 (2010).

[4] H. Zhang, W. Zhou, J. Yang, X. Li and J. Tan, J. Optoelectron. Laser **22**, 1483 (2011). (in Chinese)

[5] C. T. Zheng, C. S. Ma, X. Yan, X. Y. Wang and D. M. Zhang, Opt. Commun. **281**, 5998 (2008).

[6] C. T. Zheng, C. S. Ma, X. Yan, X. Y. Wang and D. M. Zhang, J. Mod. Opt. **56**, 615 (2009).

[7] C. T. Zheng, C. S. Ma, X. Yan, X. Y. Wang and D. M. Zhang, Opt. & Laser Technol. **42**, 457 (2010).

[8] C. T. Zheng, C. S. Ma, Z. C. Cui, X. Yan, D. M. Zhang and C. W. Tian, Opt. Quant. Electron. **42**, 327 (2011).

[9] C. T. Zheng, C. S. Ma, X. Yan, Z. C. Cui and D. M. Zhang, Appl. Phys. B **102**, 831 (2011).

[10] C. T. Zheng, C. S. Ma, X. Yan, X. Y. Wang and D. M. Zhang, Appl. Phys. B **96**, 95 (2009).

[11] C. T. Zheng, C. S. Ma, X. Yan, X. Y. Wang and D. M. Zhang, Appl. Phys. B **98**, 511 (2010).

[12] M. Lee, H. E. Katz, C. Erben, D. M. Gill, P. Gopalan and J. D. Heber, Science **298**, 1401 (2002).

[13] S. Michel, J. Zyss, I. Ledoux-Rak and C. T. Nguyen, Proceedings of SPIE **7599**, 759901 (2010).

[14] Y. Eikichi, N. Yoshiki and A. Kazuhiko, MTT-S International Microwave Symposium Diqest **3**, 119 (1983).

[15] N. H. Zhu, W. Qiu, E. Y. B. Pun and P. S. Chung, IEEE Transactions on Microwave Theory and Techniques **45**, 288 (1997).

[16] M. Balakrishnan, M. Faccini, M. B. J. Diemeer, E. J. Klein, G. Sengo, A. Driessen, W. Verboom and D. N. Reinhoudt, Appl. Phys. Lett. **92**, 153310 (2008).